Vol. 15 No 1 2009

JOURNAL OF THE BALKAN TRIBOLOGICAL ASSOCIATION

Editorial Board

Honorary and Founding Editor
Prof. Dr. Nyagol Manolov, Bulgaria

Editor-in-Chief
Prof. Dr. Slavi Ivanov, Bulgaria

Editor
Assoc. Prof. Dr. Zh. Kalitchin, Bulgaria

Associate Editors
Prof. Dr. Niculae Napoleon Antonescu, Romania
Prof. Dr. Eng. habil. K.-D. Bouzakis, Greece
Prof. Dr. Branko Ivkovič, Serbia
Prof. Dr. Mehmet Karamis, Turkey
Assoc. Prof. Dr. Mara Kandeva, Bulgaria
Assoc. Prof. Dr. V. Gecevska, FYR Macedonia

International Editorial Board
Prof. Dr. Vassil Alexandrov, Bulgaria
Prof. Dr. Vladimir Andonovic, FYR Macedonia
Prof. Dr. Miroslav Babič, Serbia
Prof. Dr. E. Diaconescu, Romania
Prof. Dr. I. Dombalov, Bulgaria
Assoc. Prof. Dr. Georgi Cholakov, Bulgaria
Prof. Dr. G. Haidemenopoulos, Greece
Assoc. Prof. Dr. Mikolai Kuzinovski, FYR Macedonia
Prof. Dr. S. Mitsi, Greece
Prof. Dr. Mitko Mihovski, Bulgaria
Assoc. Prof. Dr. Durmud Odabas, Turkey
Prof. Dr. A. Michailidis, Greece
Prof. Dr. D. Pavelescu, Romania
Prof. Dr. Alexandar Rač, Serbia
Assoc. Prof. Dr. Burhan Selcuk, Turkey
Prof. Dr. Andrei Tudor, Romania
Prof. Dr. G. E. Zaikov, Russia

Scientific Bulgarian Communications Ltd., Co.

Journal of the Balkan Tribological Association

CONTENTS

Vol. 15, No 1, 2009

Overall tribology
G. PETROPOULOS, N. VAXEVANIDIS, C. PANDAZARS, A. KOUTSOMICHALIS. Postulated Models for the Fractal Dimension of Turned Metal Surfaces 1

Coatings
K.-D. BOUZAKIS, N. MICHAILIDIS. Coatings' and Other Materials' Mechanical Properties Considering Different Indenter Tip Geometries and Calibration Procedures 10

Special materials
I. TSIAFIS, K.-D. BOUZAKIS, N. MICHAILIDIS. Determination of Epoxy Resins' Mechanical Properties by Experimental-computational Procedures in Tension 18

Erosive wear
E. GERCEKCIOGLU, D. ODABAS, E. DAGASAN. Effect of Impact Angle on the Erosive Wear Rate of Dual-phase (DP) AISI 1020, AISI 1040, AISI 4140 and AISI 8620 Steels 25

Wear
M. BAGCI, H. IMREK. Effects of Sliding Speed in a CuZn10 Brass Material on Wear 35

Computer software for evaluation of wear of the drilling
A. NEACSA, N. N. ANTONESCU, D. B. STOICA. Software Applications for Complex Technological Systems Reliability 45

Technological tribological processes
I. NAE, N. N. ANTONESCU, M. PETRESCU. Tribomodel for the Research of the Die–Tubular Material Contact with Applications in Drilling-Extraction 52

Adhesion
A. TUDOR, N. SANDU, E. TOUNTAS. Wheel/Rail Adhesion and Analysis by Using the Amsler Machine 60

Nanoparticles preparation
E. MANOVA, D. PANEVA, B. KUNEV, I. MITOV. Mechanochemical Synthesis and Characterisation of Ni–Zn Ferrite 66

Milling tribochemistry
N. G. KOSTOVA, E. DUTKOVA, P. BALAZ. Titania–Alumina Mixed Oxides Prepared by Mechanical Milling. 72

High-energy milling tribochemistry
M. ACHIMOVICOVA, P. BALAZ, E. DUTKOVA, E. GOCK, V. SEPELAK. Mechanochemical Synthesis of Zinc Selenide 79

Porous lubricity
C. S. POPESCU, V. MARIAN, M. D. PASCOVICI. Experimental and Theoretical Analysis of the Permeability for Highly Compressible Porous Layers 86

Lubrication
M. RIPA, C. SPANU, S. CIORTAN. Characterisation of Hydraulic Oils by Shear Stability and Exptreme Pressure Tests 93

Friction of porous bearings
R. F. TUNAY, C. KURBANOGLU. Effects of Lubricating Conditions on the Friction Coefficient of Sintered Journal Bearings under Alternated Loading 103

Friction – surface roughness
E. S. TOPAL. Effect of Stepover Ratio on Surface Roughness in Flat End Milling 115

Management and organisation
I. RADULESCU. Interest in Life-cycle Management for Developing an Integrated Informational Network in Lubrication Domain 123

Information
G. E. ZAIKOV, L. L. MADYUSKINA. Bio and Polymers. New Polymer Technologies with Water 132
G. E. ZAIKOV, L. L. MADYUSKINA. FAO/ESCORENA 2008 International Conference on Flax and Other Bast Plants 135

Journal of the Balkan Tribological Association *Vol. 15, No 1, 25–34 (2009)*

EFFECT OF IMPACT ANGLE ON THE EROSIVE WEAR RATE OF DUAL-PHASE (DP)AISI 1020, AISI 1040, AISI 4140 AND AISI 8620 STEELS

E. GERCEKCIOGLU[a]*, D. ODABAS[a], E. DAGASAN[b]

[a] *Engineering Faculty, Department of Mechanical Engineering, Erciyes University, 38 039 Kayseri, Turkey*

[b] *Engineering Faculty, Department of Materials Science and Engineering, Erciyes University, 38 039 Kayseri, Turkey*

E-mail: gercek@erciyes.edu.tr; odabasd@erciyes.edu.tr; edagasan@erciyes.edu.tr

ABSTRACT

In this study the effect of impact angle on the erosive wear behaviour of dual-phase steels was explored by using low carbon and low alloyed AISI 1020, AISI 1040, AISI 4140 and AISI 8620 steels. The homogenised and normalised specimens of these different steels were intercritically annealed at 780°C for 20 min and then quenched in a brine solution at –10°C. After heat treatment steps erosive wear tests were carried out at 6 different impact angles including 15, 30, 45, 60, 75 and 90° at constant particle velocity of 30 m/s. During erosive wear tests 420 μm-sized G40 particles were used as erodent and particles were blown for 240 s. As a result it was observed that martensite volume fraction of the steels increased with increasing carbon content of the steel and also erosive wear rate of used steels increased by decreasing impact angle.

Keywords: erosive wear, dual-phase steels, impact angle, AISI 1020, AISI 1040, AISI 4140, AISI 8620.

AIMS AND BACKGROUND

Dual-phase steels are new and special kinds of high strength low alloyed steels (HSLA). Steels in this class can be characterised by a tensile strength of 550 MPa and by a microstructure that consists of 15–20% hard martensite particles dispersed in soft and ductile ferrite matrix[1]. The dual-phase term refers to the existence of two main phases in the microstructure: martensite and ferrite.

* For correspondence.

However, other phases like bainite, pearlite and retained austenite may also be present in the microstructure due to the annealing temperature, annealing time and cooling rate[1–5]. This microstructure presents some characteristic properties like continuous yielding behaviour and higher total elongation than other HSLA steels that provide the same strength[6,7].

Because of their low yield strength/tensile strength ratios dual-phase steels have higher strength/weight parameters. Thus, they are generally used in automotive industry to decrease fuel consumption indirectly by decreasing total vehicle weight[2,8].

In recent years dual-phase steels are attracting interest not only of their improved mechanical properties, but also of their simple and basic production processes. Dual-phase microstructures can be easily obtained by 2 steps of heat treatment which are called intercritical annealing and quenching[1–3]. At intercritical annealing step, ferritic-pearlitic steels are annealed between A_1 and A_3 temperatures (at the ferrite + austenite region). Thus, pearlite in the starting microstructure transforms into austenite. At this point, intercritical annealing time is not an independent parameter. It is a function of the thickness and the chemical content of the specimen[2,3].

The second step of the dual-phase heat treatment is generally known as 'quenching'. At this step intercritically annealed specimens are cooled rapidly. By this way, austenite transforms to martensite. At last, a final microstructure that consists of ferrite and martensite is obtained with different volume fractions of martensite (MVF) that depend on the parameters like intercritical annealing temperature (ICAT), intercritical annealing time and cooling rate[1–3].

On the other hand, erosive wear is a well-known and a wide spread kind of wear. Generally erosive wear on solid materials consists of sliding, ploughing or impact effects of solids, fluids, gases or combination of them[9,10]. Bitter[9] determined erosive wear as a combined process of repeated deformation and cutting. During erosive wear, the surface roughness may increase because the impinging particles may remove material from lower points on the surface.

Erosive wear rate of the materials is a complex function of several parameters like target material (mechanical properties and microstructure of the target material), particle velocity, impact angle, erodent particle size and the shape of erodent particles[11,12].

The relation between erosive wear rate and impact angle is generally determined by the properties of the target material[12]. Ductile materials like metals and alloys show maximum erosive wear rate at intermediate impact angle values like 15, 30°, and brittle materials (glass, etc.) generally show maximum erosive wear rates at right angle[9,13]. That is because of the change in wear mechanism from microcutting and/or microploughing to microcracking as the impact angle increases to 90° (Ref. 14). Cutting process was attributed to particles

striking the solid surface at an acute angle and scratching out some material from the surface[9,13,14].

EXPERIMENTAL

Materials. During experimental study 4 different steels with different carbon contents were used to explore the effect of impact angle on the erosive wear rate of dual-phase microstructure. The chemical compositions of the steels used during experimental study are given in Table 1.

All steels were received in the form of 30 mm diameter cylindrical bars.

Table 1. Chemical compositions of steels used (wt. %)

Steel	C	Si	Mn	Ni	Cr	Mo	Fe
AISI 1020	0.18	0.19	0.60	0.55	0.020	0.002	balance
AISI 1040	0.36	0.25	0.65	0.06	0.002	0.002	balance
AISI 4140	0.41	0.22	0.65	0.00	1.100	0.220	balance
AISI 8620	0.25	0.27	0.94	0.53	0.570	0.210	balance

Heat treatment procedure. Figure 1 shows the schematic view of all heat treatment steps.

As-received cylindrical bars of all steels were firstly homogenised at 1170°C for 5 h and furnace cooled. As the second step of heat treatment path, homogenised bars of AISI 1020 and AISI 8620 steels were normalised at 910°C for 30 min while AISI 1040 and AISI 4140 bars were being normalised at 880°C for 30 min. All of the steels were air-cooled after normalisation.

Before dual-phase heat treatment steps critical temperatures of all steels were determined from the Andrews' basic formula (equations (1) and (2)) as can be seen from Table 2.

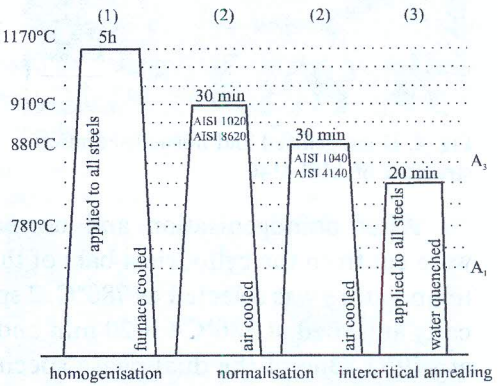

Fig. 1. Schematic view of heat treatment steps

$$Ac_3 = 910 - 203\sqrt{C} - 15.2Ni + 44.7Si + 104V + 31.5Mo + 13.1W \quad (1)$$

$$Ac_1 = 723 - 10.7Mn - 16.9Ni + 29.1Si + 16.9Cr + 290As + 6.38W \quad (2)$$

Table 2. Critical temperatures of steels

Steel	A_1 (°C)	A_3 (°C)
AISI 1020	727	832
AISI 1040	723	800
AISI 4140	741	796
AISI 8620	715	831

Figures 2–5 show micrographs of the homogenised and normalised microstructure of AISI 1020, AISI 1040, AISI 4140 and AISI 8620, respectively.

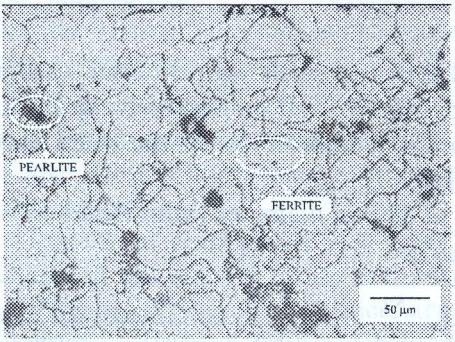

Fig. 2. Homogenised and normalised microstructure of AISI 1020

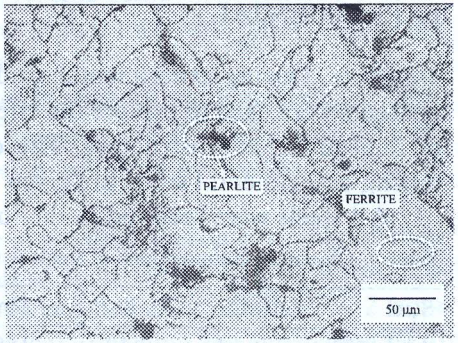

Fig. 3. Homogenised and normalised microstructure of AISI 1040

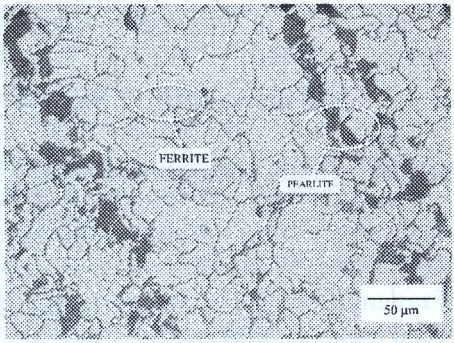

Fig. 4. Homogenised and normalised microstructure of AISI 4140

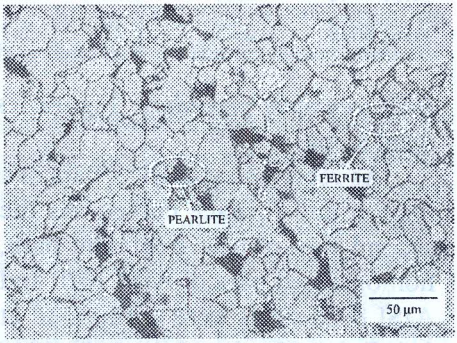

Fig. 5. Homogenised and normalised microstructure of AISI 8620

After homogenisation and normalisation steps, 2 mm-thick specimens were cut from the cylindrical bars of the steels. For all steels a constant critical temperature was selected as 780°C. 2 specimens from each steel were intercritically annealed at 780°C for 20 min and then quenched in a 10% brine solution at –10°C. One of the dual-phase specimens was used for metallographical explores and the other one – for erosive wear tests.

Metallographic studies and calculation of MVFs. After intercritical annealing and quenching all of the specimens were polished and etched with Nital 2 and then their surfaces were cleaned with acetone. The dual-phase microstructures of AISI 1020, AISI 1040, AISI 4140 and AISI 8620 specimens are given in Figs 6–9, respectively.

In order to compare the martensite volume fractions (MVF) of steels with different chemical contents, 15 images were taken from different parts of each

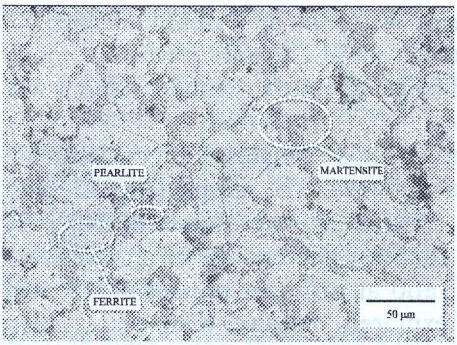

Fig. 6. Dual-phase microstructure of AISI 1020

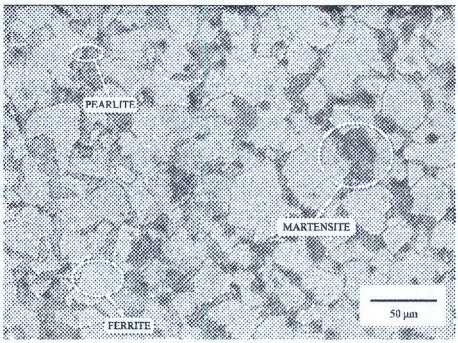

Fig. 7. Dual-phase microstructure of AISI 1040

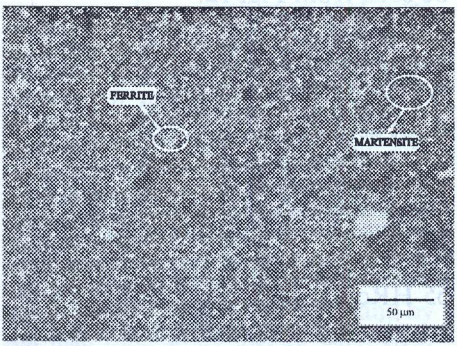

Fig. 8. Dual-phase microstructure of AISI 4140

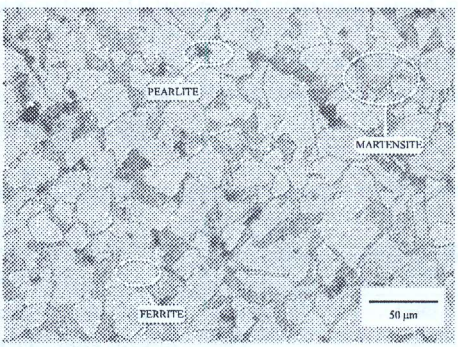

Fig. 9. Dual-phase microstructure of AISI 8620

specimen and these images were processed by Image ProPlus®. Image processing and point counting steps can be seen in Figs 10 and 11.

The determined MFVs of the used steels can be seen in Table 3.

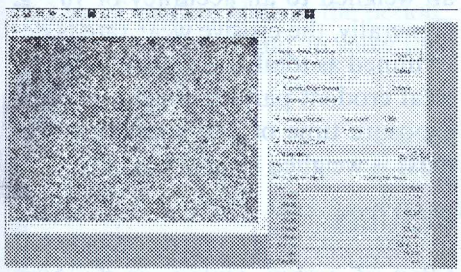

Fig. 10. Point counting with Image ProPlus®

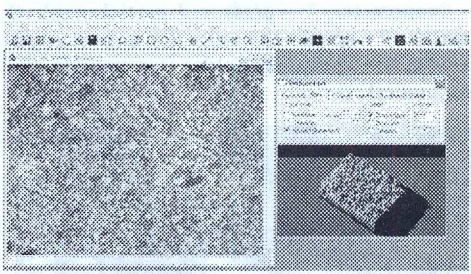

Fig. 11. Distribution of phases on Image ProPlus®

Table 3. Change of MVF with the carbon content of the steel

Steel	Carbon content (%)	MVF (%)
AISI 1020	0.18	17
AISI 1040	0.36	28
AISI 4140	0.41	35
AISI 8620	0.25	21

Erosive wear test system and erodent particles. After the dual-phase microstructure obtained erosive wear tests were carried out at constant particle velocity of 30 m/s. Particle velocity was controlled by gas pressure regulators and it was measured by using double-disc method.

Each specimen was eroded at 6 different impact angles that consist of 15, 30, 45, 60, 75 and 90° by changing the orientation of the sample (Fig. 12) with constant exposure times of 240 s. By this way the change in erosive wear ratio at different impact angles was explored. Erosive wear test system used during experimental study can be seen from Fig. 12.

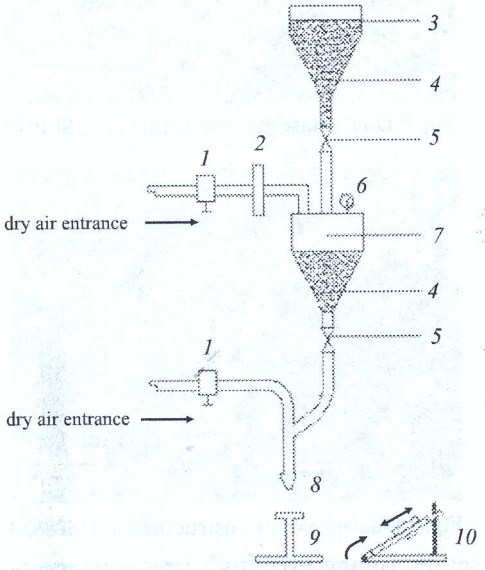

Fig. 12. Schematic view of erosive wear test system *1* – pressure regulators, *2* – powder filter, *3* – mean reservoir, *4* – erodent particles, *5* – valves, *6* – manometer, *7* – pressured particle tank, *8* – nozzle, *9* – specimen holder (for impact angle of 90°), *10* – specimen holder (for smaller impact angles)

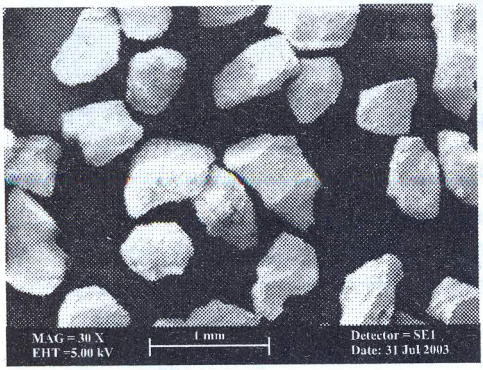

Fig. 13. SEM of G40 erodents

In the test system the nozzle diameter and the distance between the nozzle and the specimen were constant as 6 and 10 mm, respectively.

During erosive wear tests 420 μm-sized G40 particles were used as erodent. The SEM micrograph of the particles is given in Fig. 13. G40 have 55 HRc hardness with uniform martensitic microstructure and a density of 7.2 g cm.

After erosive wear tests, the samples were cleaned with low-pressure air, washed with alcohol and they were all weighed to an accuracy of 10^{-5} g. Generally, the erosive wear rate is determined as total mass loss divided by total erodent particle weight. For the exposure time of 240 s total erodent mass is weighed as 58.2 kg.

RESULTS

Effect of carbon content on the martensite volume fraction. The change in martensite volume fractions with the carbon content of the used steels is given in Fig. 14. After dual-phase heat treatments it was observed that dual-phase AISI 4140 specimens which have maximum carbon contents of the

steels used have the maximum martensite volume fraction values, too.

Anyway as can be easily seen from Fig. 14, martensite volume fractions of steels increase with increasing carbon content because of the increase in carbon content that dissolves in austenite during intercritical annealing.

Effect of impact angle on the total mass loss and erosive wear rate. Dual-phase specimens from each steel that were intercritically annealed at 780°C and rapidly quenched in the same solution were eroded at 6 impact angles by using 2 different holders that can be seen in Fig. 12. Table 4 shows constant parameters during erosive wear tests.

All specimens were weighed before and after erosive wear tests and by the way total mass loss of each steel determined. After then total mass losses were divided by total erodent mass to find out erosive wear rate. For such a system seen in Fig. 12, totally 58.2 kg of erodent blow in the period of 240 s. Figures 15 and 16 show the

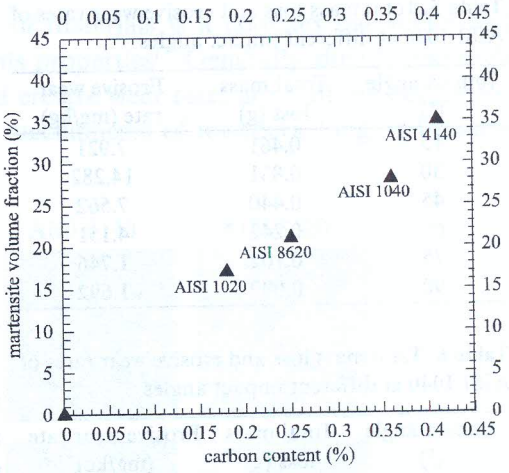

Fig. 14. Change of MVF with the carbon content of the steel

Table 4. Constant parameters during erosive wear tests

Parameter	Value
Erodent particles	G40
Particle tank pressure (bar)	2
Nozzle diameter (mm)	7
Nozzle length (mm)	10
Distance between the nozzle and specimen (mm)	10
Particle velocity (m/s)	30
Air entrance pressure (bar)	2
Exposure time (s)	240

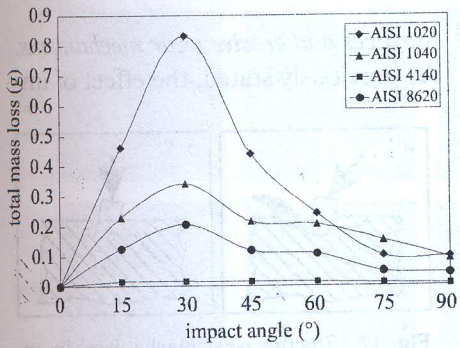

Fig. 15. Change of total mass loss with the impact angle

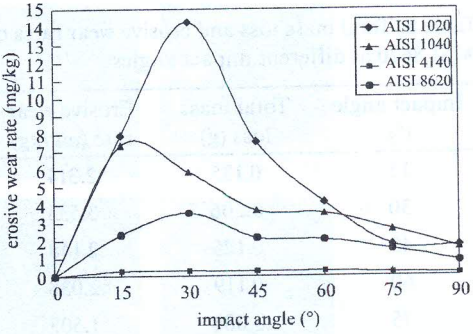

Fig. 16. Change of erosive wear rate with the impact angle

Table 5. Total mass loss and erosive wear rates of AISI 1020 at different impact angles

Impact angle (°)	Total mass loss (g)	Erosive wear rate (mg/kg)
15	0.461	7.921
30	0.831	14.282
45	0.440	7.562
60	0.242	4.151
75	0.102	1.746
90	0.099	1.692

Table 6. Total mass loss and erosive wear rates of AISI 1040 at different impact angles

Impact angle (°)	Total mass loss (g)	Erosive wear rate (mg/kg)
15	0.429	7.371
30	0.341	5.852
45	0.215	3.691
60	0.206	3.533
75	0.153	2.622
90	0.092	1.584

Table 7. Total mass loss and erosive wear rates of AISI 4140 at different impact angles

Impact angle (°)	Total mass loss (g)	Erosive wear rate (mg/kg)
15	0.016	0.274
30	0.017	0.292
45	0.016	0.273
60	0.017	0.292
75	0.011	0.196
90	0.008	0.141

Table 8. Total mass loss and erosive wear rates of AISI 8620 at different impact angles

Impact angle (°)	Total mass loss (g)	Erosive wear rate (mg/kg)
15	0.135	2.314
30	0.206	3.533
45	0.125	2.148
60	0.119	2.038
75	0.088	1.503
90	0.049	0.842

change in total mass and erosive wear rate of each steel by the impact angle, respectively.

Tables 5–8 show the total mass loss and erosive wear rate of dual-phase AISI 1020, AISI 1040, AISI 4140 and AISI 8620 steels at each impact angle, respectively.

The data of Figs 15 and 16 show that:

1. All steels have their maximum mass losses and erosive wear rates at an impact angle of 30° and both of these values decrease with increasing impact angle, due to the change in erosive wear mechanism from microcracking to microcutting and/or microploughing as the impact angles go from 90° to smaller.

2. On the other hand, there is a significant point that the mass loss and erosive wear rate values of all steels reach their maximum values at 30° instead of 15°, because of the position of the angular specimen holder seen in Fig. 12. At an impact angle of 15°, some of the particles do not touch the specimens surface at that position.

Surfaces and erosive wear mechanisms. As previously stated, the effect of im-

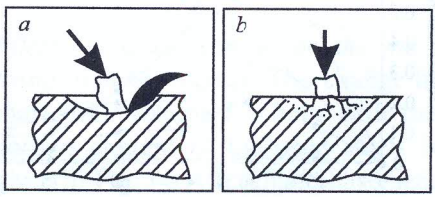

Fig. 17. Effective wear mechanisms in angular and right impact[9]

pact angle on the erosive wear rate of materials is a complex parameter and mostly depends on the target materials properties[13]. Generally, ductile materials have their maximum mass losses and erosive wear rates at small impact angles. Figure 17 schematically shows wear mechanisms of microcracking and micro-ploughing.

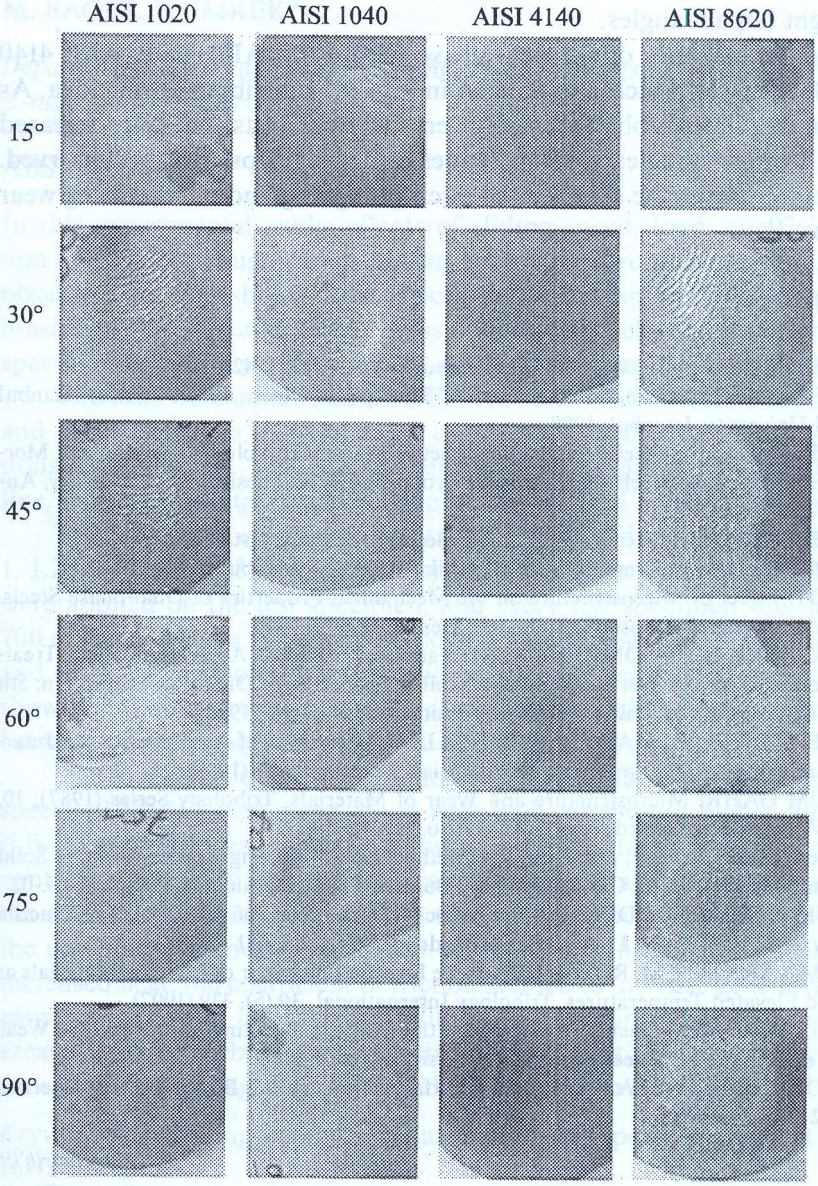

Fig. 18. View of surfaces after erosive wear tests

According to Tables 5–8, it is obvious that under angular impact conditions dual-phase steels behave like ductile materials. They have their maximum erosive wear rates at an impact angle of 30°.

Generally, during erosive wear processes of ductile materials under small impact angles, microploughing and microcutting mechanisms are effective while erosive wear processes are being controlled by microcrakcing mechanisms at right impact angles.

Final surface shapes of the dual-phase AISI 1020, AISI 1040, AISI 4140 and AISI 8620 steels, which can be seen in Fig. 18, contribute to this idea. As can be seen in photographs taken after erosive wear tests that were released under small impact angles surface shapes called as 'rips' can be observed. That formation proves the existence of microploughing and microcutting wear mechanisms.

REFERENCES

1. G. R. SPEICH: Dual-phase Steels. ASM Handbook, Vol. 1, 1993, 424–429.
2. H. CIMENOGLU: Deformation Behavior of Dual-phase Steels. Ph.D. Thesis, Istanbul Technical University, Istanbul, 1988.
3. B. DEMIR: Dual-phase Steel Production, Effect of Martensite Volume Fraction and Morphology of Dual-phase Steels on the Tensile Properties. MsC Thesis, Gazi University, Ankara, 1997.
4. T.-E. THELNING: Heat Treatment of Steels. Bofors Handbook, Istanbul, 1984.
5. M. A. TOPBAS: Heat Treatments. Yildiz Teknik University, Istanbul, 1993.
6. M. AKSOY: Effect of Microstructure on the Mechanical Properties of Dual-phase Steels. Part 3. In: Materials Symposium in Denizli, Denizli, 1989, 33–44.
7. A. BAKKALOGLU, N. SONMEZ: Determination of the Most Appropriate Heat Treatment Parameters for the Best Strength–Formability Properties of Dual-phase Steels. In: 5th National Congress on Machine Design and Production, Ankara, 1992.
8. G. R. SPEICH, V. A. DEMAREST, R. L. MILLER: Formation of Austenite during Intercritical Annealing of Dual-phase Steels. Metarials Transaction A (1981).
9. K. H. ZUM GAHR: Microstructure and Wear of Materials. Tribology Series (1987), 10, Elsevier, Amsterdam–Oxford–New York–Tokyo, 1987, 531–558.
10. ASTM Designation: G76-95, Standard Test Method for Conducting Erosion Tests by Solid Particle Impingement Using Gas Jets. Annual Book of ASTM Standards (2000), Vol. 03.-02.
11. I. FINNIE, D. H. McFADDEN: On The Velocity Dependence of the Erosion of Ductile Metals by Solid Particles at Low Angles oflncidence. Wear, **48**, 181 (1978).
12. G. SUNDARARAJAN, M. ROY: Solid Particle Erosion Behaviour of Metallic Materials at Room and Elevated Temperatures. Tribology International, **30** (5), 339 (1997).
13. K. YILDIZLI: An Experimental Research on the Effect of Boriding on the Erosive Wear Behavior of Steels. MsC Thesis, Erciyes University, Kayseri, 2002.
14. K. FRIEDRICH: Erosive Wear of Polymer Surfaces by Steel Ball Blasting. J. of Materials Science, **21**, 3317 (1986).